Identification of a Continuous Microhertz Signal Consistent with Gravitational Radiation from Zeta Phoenicis

Herbert Weidner,[1]★
[1] *University of applied sciences, Aschaffenburg, Germany*

Accepted XXX. Received YYY; in original form ZZZ

ABSTRACT

We investigate whether long-term atmospheric pressure measurements contain a coherent, frequency-stable signal consistent with the expected gravitational-wave (GW) emission from the eclipsing binary Zeta Phoenicis. The system's orbital period of 1.6697739 days implies a GW frequency of 13.863 μHz, a regime inaccessible to conventional interferometric detectors. Using 20 years of hourly pressure data from more than 100 stations, we apply a communications-engineering approach combining coherent integration, superheterodyne frequency shifting, and iterative phase-demodulation to isolate weak, structured oscillations. After compensating for frequency drift and multiple phase modulations, we recover a narrow, persistent spectral feature at the predicted frequency. One modulation matches the annual Doppler signature expected from Earth's orbital motion, while additional low-frequency sidebands may reflect longer-period dynamical influences within the source system. We further derive a long-term decrease in the GW frequency, corresponding to a secular increase in the orbital period, and provide a prediction for the period in 2026. These results demonstrate that phase-sensitive demodulation techniques can extract ultra-low-frequency, coherent signals from noisy geophysical data and may offer a complementary pathway for probing continuous GW sources in the microhertz regime.

Key words: Data Methods – Zeta Phoenicis – Low frequency – Gravitational wave

1 INTRODUCTION

Gravitational waves (GWs) are a fundamental prediction of general relativity, and binary stars are expected to emit continuous radiation at twice their orbital frequency. For systems with periods of order days, the corresponding GW frequencies fall in the microhertz regime – far below the sensitivity range of ground-based interferometers, which are limited to frequencies above several tens of Hertz. Consequently, the ultra-low-frequency GW domain remains largely unexplored, despite the abundance of nearby eclipsing binaries that should, in principle, contribute measurable signals.

Zeta Phoenicis is an Algol-type eclipsing binary with an orbital period of 1.6697739 days. Its expected GW frequency of 13.863 μHz lies in a spectral region where conventional detection techniques are ineffective, and where long-term geophysical measurements exhibit several unexplained narrow features. Atmospheric pressure records, in particular, contain persistent spectral lines whose origin is not yet understood and which motivate a closer examination of this frequency range.

In this work, we investigate whether long-baseline atmospheric pressure measurements contain a coherent, frequency-stable component consistent with the expected GW signal from Zeta Phoenicis. To this end, we adopt a communications-engineering approach: we construct a receiver tuned to the predicted emission frequency, treat terrestrial sensors as effective antennas, and apply phase-sensitive demodulation and coherent integration techniques to extract weak, structured signals from noise. This methodology allows us to probe frequency drifts, annual Doppler modulations, and additional low-frequency sidebands that may encode dynamical information about the source system.

Our aim is to assess whether the observed spectral feature at 13.863 μHz can be attributed to a continuous astrophysical signal and to characterize its temporal behaviour, including potential modulations arising from orbital motion within the *Zeta Phoenicis* system.

2 MYSTERIOUS SIGNAL SOURCES

When a celestial body or a GW deforms the Earth, pressure changes and accelerations occur on the surface. Sensitive sensors convert these into electrical signals, which we examine. The longer the measurement period T_{min}, the lower the frequency uncertainty Δf. According to Küpfmüller (1993), the following applies:

$$T_{min} \cdot \Delta f \geq 0.5 \tag{1}$$

With a minimum period of $T_{min} > 20$ years, we reach the value $\Delta f \approx 0.8$ nHz. The atmospheric pressure spectrum (Figure 1) shows several lines of unclear origin. One of these lies at the frequency at which we expect the GW of the binary star system *Zeta Phoenicis*. Neighboring celestial bodies such as the Moon also produce spectral lines, which are listed in Hartmann (1995). The closest interfering frequencies are found there at 13.81 μHz and 13.90 μHz – far outside the range shown.

★ herbertweidner@gmx.de

© 2026 The Authors

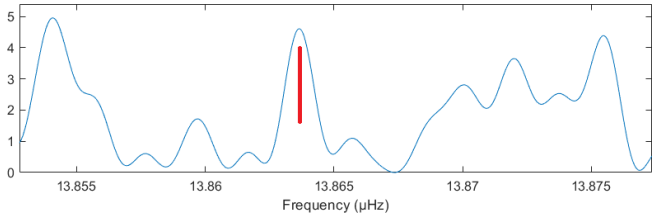

Figure 1. Power spectrum of the atmospheric pressure, one measurement per hour. The data is based on the average pressure in Germany between 2000 and 2020. The red bar marks f_{GW} of *Zeta Phoenicis*.

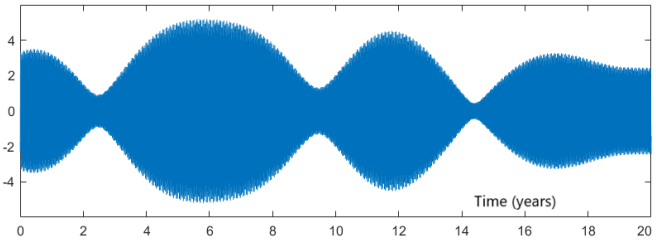

Figure 2. Total amplitude of the frequency mixture in the range ($13.858 < f < 13.868$) μHz as a function of time. The signal-to-noise ratio is surprisingly good considering the questionable 'antenna'. Cutting off all higher sideband frequencies with $f_{modulation} > 5$ nHz can distort the envelope, but improves the signal-to-noise ratio (SNR).

It is unclear what sources generate the spectral lines in this frequency range. Below 20 μHz, the amplitude in the spectrum increases approximately proportionally to f^{-3} (Weidner 2025). If this were noise, one would expect a fall-off proportional to f^{-1} (Colors of noise 2026). Apparently, there are numerous, as yet unknown sources causing this inexplicable increase. This phenomenon is reason to investigate a narrow spectral range and identify possible sources. Short-term phenomena such as ocean-atmosphere coupling, Chandler wobble, and annual modes cannot generate waves that are detectable with extreme frequency stability for over 20 years.

Barometers are not the only devices that react to these special waves: We found almost identical spectra in the records of superconducting gravimeters. However, two factors impair the quality: no gravimeter has been operated continuously for decades (resulting in broadened spectral lines), and frequent earthquakes increase the noise level. Although the two measurement methods differ fundamentally, they produce strikingly similar spectra. The cause is apparently a common one – possibly GW. We will not discuss this question in this paper. Our sole focus is on reception technology and signal analysis.

3 THE CHOICE OF BANDWIDTH

We suspect that radiation from binary stars is the cause of the peculiar amplitude increase in the spectrum. Binary stars are very common in our galaxy, and many of them may have planetary systems. If this assumption applies to *Zeta Phoenicis*, the planets force the binary system to move around the center of gravity of the entire system. Then the generated GW is phase-modulated and accompanying frequencies arise on both sides of f_{GW} (sidebands). The orbital radii of the planets determine the modulation frequencies, the masses determine the modulation indices. Since the orbital period of the binary system can change over time (drift), the bandwidth (BW) of the receiving channel should significantly exceed the minimum value $\Delta f \approx 0.8$ nHz. It is difficult to determine BW without prior knowledge of the overall system. Too high a value increases the noise level and impairs reception quality. A value that is too small will delete or distort possible modulations (see sector 12.3).

In Figure 1 are two weak, symmetrical spectral lines at a distance of 2 nHz from f_{GW}. Whether these are sidebands generated by modulation of f_{GW} cannot be determined because the spectrum erases all phase information. The answer requires subtle methods of communications engineering, which we will discuss below.

Albert Einstein believed that GWs were practically immeasurable due to their low amplitude. In fact, no prominent spectral lines that could be generated by GWs can be found in any spectrum or frequency range. This changes when long periods of time are considered and BW is reduced to improve the signal-to-noise ratio. At a bandwidth of 10 nHz, we see an obviously modulated continuous signal instead of the expected noise (Figure 2). Is it the GW from *Zeta Phoenicis*? We emphasize that no source in the solar system generates this signal because Hartmann (1995) contains no corresponding entry in this frequency range. This frequency gap is the only reason to analyze the GW of *Zeta Phoenicis* and not the GW of the closer binary star *Algol*: The moon causes tides on Earth. One of these has almost the same frequency as the GW from Algol, and the two are difficult to separate. The limitation to BW = 10 nHz has consequences:

Figure 2 gives the impression of an amplitude-modulated oscillation. This is probably an artifact: The arbitrarily chosen BW suppresses sideband frequencies outside the BW and therefore distorts the information transported there. The actual envelope and modulation requires a detailed data analysis, including all relevant sidebands and adjustment of the BW.

During the measurement period, the Earth orbits the Sun 20 times. If the signal source is not located near one of the two poles of the ecliptic, our distance from the source changes periodically. The Earth moves toward or away from *Zeta Phoenicis* at a maximum speed of 17.3 km/s. Due to the Doppler effect, the reception frequency f_{GW} should fluctuate periodically by a maximum of ±0.8 nHz (Figure 7). This value is referred to as the frequency deviation of the frequency or phase modulation. A property of this type of modulation that is not easy to understand but has been experimentally verified is that it is not the frequency deviation that appears in the spectrum, but two sideband frequencies at a distance of ±31.69 nHz from f_{GW}. The distance is the modulation frequency (reciprocal of the length of the year), and the amplitude is a measure of the frequency deviation.
If we suppress these signal components beyond the selected bandwidth in order to minimize noise, we delete the information necessary to detect the periodic annual modulation.

We only examine the immediate vicinity of the unchanged spectral line at f_{GW}. The selected bandwidth allows us to detect frequency drift and slow modulations of the signal at frequency f_{GW} when $f_{mod} < 5$ nHz. This allows us to detect planets with orbital periods longer than 6.3 years.

4 COHERENT SIGNAL INTEGRATION

Communications engineering knows several methods for detecting a signal of defined frequency in a frequency mixture. One is the coherent addition of successive oscillations, taking into account the phase relationship. The method can be summarized as follows (section 12.1): An oscillator oscillates at the desired frequency with a

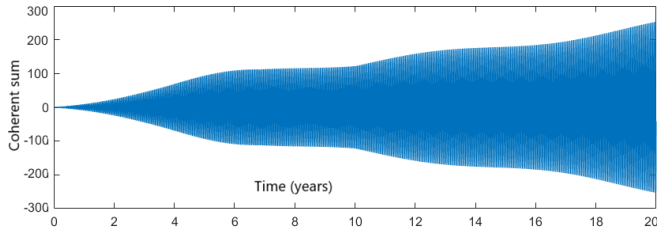

Figure 3. Coherent sum of the signal from figure 2 as a function of time. The resonator responds preferentially to its resonant frequency 13.863 μHz.

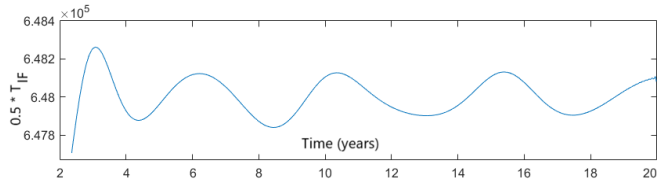

Figure 4. A frequency-modulated signal causes the oscillation period of the intermediate frequency to oscillate around the target value of 648,000 seconds (injection pulling). The results of the first two years are omitted because the small amplitude of the coherent sum does not allow for a precise determination of the oscillation period.

certain amplitude. If it is disturbed by an injected signal, it reacts in a characteristic manner:

If the injected signal mixture contains the desired frequency, the amplitude of the oscillator increases or decreases depending on the phase difference. This disappears after a sufficiently long time (injection locking).

With an unmodulated signal of the same phase, the coherent sum increases proportionally to time.

Signals of similar frequency cause injection pulling. The frequency of the oscillator follows the signal frequency within certain limits. This can lead to a ripple in the smooth envelope (Figure 3) or to a periodic frequency change (Figure 4).

Signals with poor SNR usually exhibit high phase noise. Injection locking provides a means to significantly reduce phase noise.

Interference pulses are always broadband and can be effectively suppressed by an upstream band filter.

Figure 3 shows the result for a very narrow frequency range around 13.863 μHz. The almost linear increase in the envelope shows that the frequency and amplitude of the carrier frequency hardly change during the entire 20-year measurement period. Weak signals (sidebands) of high frequency stability within the selected bandwidth modulate the envelope.

5 SUPERHET

We suspect the double star *Zeta Phoenicis* to be the source of the signal described above. The frequency f_{GW} could change slowly (drift), and existing planets cause phase modulation (PM). The aim of our research is to determine the exact value of f_{GW}, the frequency drift, and possible PM. We must eliminate these peculiarities of the signal by means of an intermediate step, because the coherent signal integrator expects an unmodulated signal of constant frequency. With a modified superheterodyne, we can shift the reception channel to a lower frequency f_{IF} and simultaneously eliminate the modulations. We achieve this by modulating a local oscillator of the intermediate frequency f_{loc} in the same way as the signal coming from the antenna. The better the copy, the more constant the difference frequency f_{IF} is. We check this by determining the oscillation period of f_{IF} by counting. If the oscillation period oscillates around a mean value as in Figure 4, the signal is frequency-modulated. We can estimate the modulation frequency, modulate the local oscillator with it, and start a new iteration. Due to a lack of information, we have to guess the frequencies at which the GW signal could be (phase) modulated.

We start with the usual approach

$$y = sin(2\pi t \cdot f_{signal} + \phi_{modulation}) \tag{2}$$

and adjust the two parameters f_{signal} and $\phi_{modulation}$ to the problem: The frequency f_{signal} can change proportionally to time and $\phi_{modulation}$ can be the sum of several sine functions. If the modulation consists of a single frequency f_{mod}, the equation is

$$y = sin(2\pi t(f_{signal} + t\dot{f}) + \eta \cdot sin(2\pi t f_{mod} + \varphi)) \tag{3}$$

A sinusoidal PM causes the instantaneous frequency of the signal to fluctuate periodically between the limits $f_{signal} + \Delta f$ (maximum blue shift) and $f_{signal} - \Delta f$ (maximum red shift). The quantity Δf is referred to as the frequency deviation. The instantaneous frequency at a given point in time is difficult and inaccurate to measure, as it is never constant over a longer period of time. It is easier and more common to determine the modulation index η using equation (3) and calculate $\Delta f = \eta \cdot f_{mod}$.

Since we are changing the signal frequency using the Superhet method, we need to adjust the approach (for a single planet):

$$f_{loc} = f_{GW} + f_{IF} + t\dot{f}_{GW} + \eta_{mod} \cdot sin(2\pi t f_{mod} + \varphi_{mod}) \tag{4}$$

If multiple planets are suspected, equation (4) is supplemented with additional summands with adjusted constants η_n, f_n and φ_n. We calculate the difference $f_{GW} - f_{local} = f_{IF}$ using the usual superheterodyne method and verify the frequency-shifted signal with coherent signal integration. If f_{IF} changes, we minimize the deviations by iterating the characteristic values of f_{loc}. After several steps, the local oscillator f_{loc} is modulated in the same way as the GW signal.

Using the superheterodyne principle, we reduce the signal frequency from f_{GW} = 13.863 μHz to a 'smooth' value, for example $f_{IF} = 1/(360 \text{ hours}) \approx 772$ nHz. Then the value of each individual oscillation can be determined with particular accuracy. With the selected value of f_{IF}, the time span between adjacent zero crossings should be exactly 648000 seconds (half the oscillation period of the intermediate frequency). The intermediate result in Figure 4 shows that there are apparently further frequency modulations. The reduced frequency allows for a longer sampling period and faster calculation.

6 RESULTS – 1 (BW = 10 NHZ)

The aim of this work is to identify the GW of *Zeta Phoenicis*. Since the frequency is likely to change slowly (drift) and the literature search (Simbad 1991) provides no clues, we initially select a large bandwidth of BW = 10 nHz. The measurements show that the choice of BW has an unexpectedly strong influence on the results (Table 1, column 3). Periodic frequency changes of f_{signal} can be detected because the corresponding sidebands lie within BW. Therefore, we also measure

Table 1. The modulations of f_{signal} = 13.863 μHz. f_1 und f_2 are the modulation frequencies of the signal. η is the individual modulation index of the phase modulations. We omit the phases φ for reasons of space.

BW (nHz)	f_{GW} (μHz)	drift $\times 10^{-20}$ s^{-2}	f_1 (nHz)	η_1	f_2 (nHz)	η_2
8	13.8636	17.6	2.14	0.614	3.84	0.216
8.2	13.8636	17.74	2.18	0.607	3.84	0.256
8.4	13.8635	23.9	2.16	0.607	3.90	0.269
8.5	**13.8626**	**180.8**	1.797	0.923	3.94	0.285
8.6	**13.8626**	**178.6**	1.81	0.910	3.94	0.305
8.7	**13.8626**	**175.8**	1.811	0.897	3.93	0.320
8.8	**13.8626**	**172.7**	1.83	0.884	3.93	0.327
8.9	**13.8626**	**169.4**	1.835	0.870	3.931	0.338
9	**13.8626**	**165.7**	1.86	0.857	3.94	0.346
9.1	**13.8627**	**162.5**	1.91	0.850	3.970	0.342
9.2	**13.8627**	**159.0**	1.90	0.834	3.96	0.363
9.3	**13.8627**	**156.6**	1.93	0.825	3.96	0.371
9.4	13.8635	339.7	1.67	1.27	4.02	0.39
9.5	13.8616	336.4	1.685	1.25	4.06	0.403
10	13.8616	329.5	1.701	1.20	4.15	0.488

these modulations by adjusting equation (4). The lowest modulation frequency is approximately 1.9 nHz. Since the oscillation period $T \approx$ 17 years is about as long as the entire measurement period (20 years), the measurement error calculated with equation (1) is enormous. An improvement would require extending the measurement period to many decades.

We define the BW using a windowed sinc filter with an rectangular passband. Small changes in BW cause sideband frequencies at the edges of BW to be switched on and off almost digitally. This changes the results abruptly in some cases (Table 1). Although smoother transitions can be achieved with other filtering methods, the basic problem remains: The bandwidth of the analysis has an unduly strong influence on the results.

Signal processing with a large bandwidth has serious disadvantages: The SNR is poor and most of the sidebands that carry valuable information are discarded. This includes, in particular, the direction of the source of the received signal. This is determined by measuring the phase shift of the Doppler shift as a result of the Earth's orbit. This measurement requires a minimum bandwidth of 64 nHz, which drastically worsens the SNR. Depending on the (initially) unknown modulation index, a significantly larger (Carson) BW may be necessary, which reduces the SNR even further.

Conclusion: We need a method that allows the signal modulations to be deciphered even with the smallest possible BW.

7 IMPROVED METHOD

We see only one way to minimize the influence of bandwidth: In a first step, we eliminate all modulations – including frequency drift. Then the signal frequency is constant and there are no sidebands that we need to consider. Another advantage is that we can filter the signal with the lowest possible BW, thereby improving the SNR. We decided on BW = 0.4 nHz (see equation (1)).

The original phase-modulated signal consists of a frequency bundle that requires a certain BW (see section 12.3). Each individual frequency within this bandwidth carries energy, but only part of the total energy of the signal is accounted for by the carrier frequency f_{GW}. If we succeed in eliminating all modulations, the total energy of the signal is concentrated in a very narrow range around f_{GW} and the SNR improves.

Every signal coming from a source outside the solar system is modulated with f_{year} = 31.69 nHz because the Earth orbits the Sun. Detecting this modulation requires a minimum signal processing bandwidth of 64 nHz. The spectrum contains evidence of fixed modulation frequencies (section 12.2), the origin of which is unclear. In the course of the investigations, it became apparent that we can only decipher all modulations without distortion with $BW \geq 2700$ nHz (Carson-BW). Such a wide frequency band contains a lot of noise and signals from other sources that degrade the SNR.

The method outlined here picks out only the frequencies that match the selected modulations and ignores all other signals within the BW. No other method has a comparably high selectivity. This method is described in Weidner (2025) and is only briefly explained here:

The preprocessor reduces the signal frequency from 13.8 μHz to 1.4 μHz without changing the modulations. The maximum possible bandwidth of the signal processing is 2.7 μHz, which is sufficient to demodulate the strongly phase-modulated signal with low distortion. Once the initial results (section 8) are known, these values can be adjusted. Extending the sampling period from one to T_s = 42 hours reduces the amount of data and the processing time.

The main loop is repeated many thousands of times:

We phase modulate the frequency of a local auxiliary oscillator with fixed frequencies f_{m1} ... f_{m5}. We have to guess the individual start values. In section 12.2, we describe a method for systematically finding modulation frequencies.

The frequency of the auxiliary oscillator and its drift are adjustable. The original assumption of a linear drift is not sufficient. The convergence improved after expanding to a quadratic drift.

We mix the signal frequency with the local auxiliary oscillator and obtain the difference frequency f_{IF}. We choose ($f_{IF} = 1/T_s/40 \approx$ 165 nHz) in order to detect even the slightest frequency changes and reduce the bandwidth of the signal processing to 0.4 nHz.

We vary the drift and modulation frequencies with two objectives: The amplitude of f_{IF} must be as high as possible and the value f_{IF} must be constant. If the errors fall below specified limits, the modulations of the auxiliary oscillator and the signal are largely identical.

The key features of this method are: We obtain a high SNR and we can measure the PM at 31.69 nHz. This allows us to determine the direction from which the signal is coming. The poor SNR of f_{signal} (Figure 1) does not allow us to determine whether the signal is amplitude-modulated.

8 RESULTS – 2 (BW = 0.4 NHZ)

Figure 5 shows that the amplitude of the intermediate frequency f_{IF} assumes considerable values because during the demodulation process, the energy of the sidebands is transferred to the carrier frequency (see section 12.3). Table 2 shows the modulations. The accuracy depends heavily on the value of the modulation frequency: For modulation-1, the measurement period of 20 years comprises approximately 74 oscillations, while for modulation-5, it is only 1.6 oscillations. This means that an estimated error of ±0.1 oscillations has a much greater impact.

We place great importance on an accurate measurement of the frequency drift because no results have been published so far. The method described in section 6 is too inaccurate, as the chosen bandwidth and low-frequency modulations influence the result. The op-

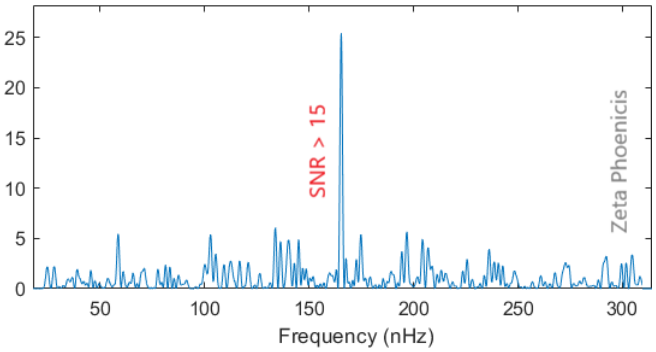

Figure 5. Power spectrum (Welch method) of the vicinity of $f_{IF} \approx 165$ nHz. The absence of symmetrical structures next to the carrier frequency means that there are no undiscovered modulations. The increase in the amplitude of the carrier frequency results from the deletion of the measured sidebands (Table 2). A comparison of the vicinity of f_{IF} with the vicinity of the signal frequency in Figure 1 is meaningless because the demodulation method (variable frequency of the local auxiliary oscillator) distorts the spectrum in the vicinity of the carrier frequency.

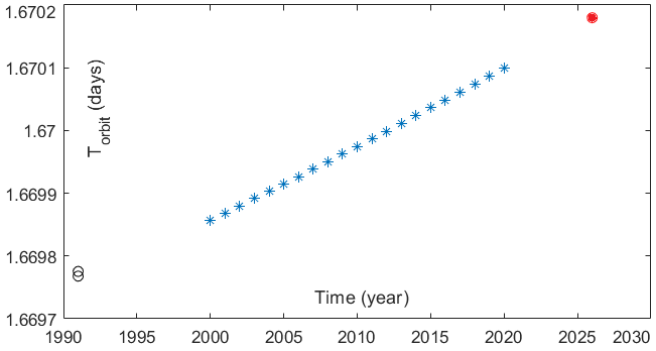

Figure 6. Orbital period of *Zeta Phoenicis* as a function of time according to equation (5) (blue stars). The two black circles at the bottom left mark earlier results (Simbad 1991). The red bullet at the top right marks our prediction for the year 2026.

posite is true for the improved method described in section 7: The intermediate frequency f_{IF} must be unmodulated and constant. The slightest changes are noticeable and the frequency drift can be determined with particular accuracy. The results:

$$f(t) = f_{signal} + t\dot{f} + t^2\ddot{f} \quad (5)$$

f_{signal} = 13.862353 ± 0.00003 μHz (Date 2020-01-01).
$\dot{f} = -2.975 \times 10^{-18} s^{-2}$
$\ddot{f} = -3.5 \times 10^{-28} s^{-3}$

The good SNR of f_{IF} (Figure 5) allows for high measurement accuracy and a prediction: The rotational frequency of the binary system decreases over time and is expected to be 13.8597 μHz in 2026. This corresponds to an orbital period of 1.67018 days.

Simbad (1991) and VizieR cite two specific results measured around 1991 as the orbital period of the binary system: P_1 = 1.6697753 days and P_2 = 1.6697678 days, without specifying any measurement errors. Figure 6 shows the measured values and the expected orbital period in 2026.

Table 2. The phase modulations of f_{signal} = 13.862353 μHz (Date: 2020-01-01). The error of the modulation frequencies Δf is estimated.

	f_{mod} (nHz)	Δf (nHz)	P (days)	φ	η
Modulation-1	118.21	±0.02	97.9	0.41	1.40
Modulation-2	31.27	±0.03	**370**	3.77	5.24
Modulation-3	28.77	±0.03	402	1.25	2.08
Modulation-4	14.37	±0.05	805	1.25	1.51
Modulation-5	1.96	±0.08	5900	6.10	2.85

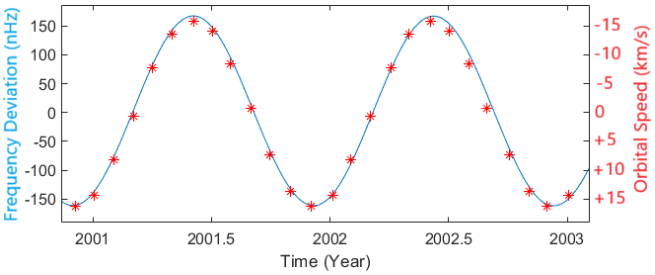

Figure 7. Comparison of the measured periodic frequency shift of f_{signal} (blue curve) with the date-dependent orbital speed of the Earth (red stars). The scale on the right has been adjusted to illustrate the good agreement. The modulation frequencies f_1, f_3, f_4 and f_5 are hidden.

9 INTERPRETATION OF THE RESULTS

We limited our measurements to the phase modulation of the signal for several reasons: a) Unlike amplitude modulation, PM exhibits the well-known phenomenon of demodulation gain with a noticeable improvement in SNR. Our measurements confirm this effect (Figure 5). b) The radiation source *Zeta Phoenicis* is located outside the solar system. Therefore, the signal must be phase-modulated with a period of 365 days. In fact, the period of phase modulation-2 (Table 2) corresponds well with the orbital period of the Earth. For the other four phase modulations, there is insufficient evidence to speculate on the causes. We suspect that this PM is caused by planets around *Zeta Phoenicis*. Below, we will only discuss the results for Modulation-2.

9.1 Direction to the source

Zeta Phoenicis is located at RA = 01 h 08 m 23 s and Dec = -55^o 14' 45". On the 153rd day of the year, the distance to *Zeta Phoenicis* decreases at a maximum speed of about 17 km/s; six months later, it increases by the same amount (Calculate radial velocities 2026). The Doppler effect causes a periodic phase change in the reception frequency, which acts like a frequency change (blueshift/redshift). Comparing the modulation phase-2 (φ_2) with the phase of the relative velocity of the Earth in Figure 7 confirms: The signal with a frequency of 13.86256 μHz comes from the same RA as the electromagnetic radiation from *Zeta Phoenicis*. To check the declination, we need the propagation speed of the wave.

9.2 Signal speed

The Doppler effect is a fundamental principle of astronomy and describes the relationship between the frequency shift Δf of the signal and the speed of the transmitter or receiver. If we assume

that the signal propagates at the speed of light c, we have to use the relativistic equation

$$\Delta f = f_{signal} \cdot \left(\sqrt{\frac{c+v}{c-v}} - 1 \right) \quad (6)$$

where v is the relative speed between the source and the Earth. For the source *Zeta Phoenicis*, the Earth's relative speed oscillates in the range -17 km s^{-1} < v < 17 km s^{-1}. This limits the Doppler shift to the range $|\Delta f| < 0.8$ nHz. We calculate frequency deviations that were 200 times higher (Figure 7). This discrepancy leaves no room for ambiguity: The propagation speed of the waves (at this frequency) is about 200 times lower than the speed of light. Similar results are found at lower frequencies around 5 μHz (Weidner 2025). The attempt to provide a theoretical foundation for v_{signal} would go beyond the context of this paper.

10 DISCUSSION

Some of our findings contradict the properties of gravitational waves predicted by A. Einstein 110 years ago. This applies in particular to the unexpectedly low propagation speed and the strong reaction of atmospheric pressure to these waves. However, we also emphasize that *continuous* GW have never been detected before. The speed of a GW has only been measured once (GW170817) and applies to frequencies above 100 Hz. We measured at a frequency millions of times lower and obtained a strongly deviating value. Future research will have to clarify whether dispersion causes this difference.

We can only partially characterize the waves received:

The 'receiving antenna' is the pressure at the interface between the atmosphere and the Earth. Apparently, the wave moves the massive globe differently than the lighter air envelope, causing periodic pressure fluctuations.

Since *Zeta Phoenicis* cannot be seen from Europe, we conclude that the mass of the Earth has little or no influence on wave propagation.

The period of the radiation from *Zeta Phoenicis* is about 20 hours, which corresponds to 5/6 of the length of a day. We have neither observed nor expected any interference from periods of 24 ± 20 hours. Corresponding measurements would require short sampling periods and significantly increase the calculation time.

Air pressure is a scalar quantity and the rotation period of the Earth is smaller than the sampling period T_s = 42 hours. Therefore, we were unable to experimentally determine whether the measured fluctuations in air pressure are caused by transverse or longitudinal waves.

Figure 6 shows that the orbital period of *Zeta Phoenicis* increases over the long term. The cause is likely to be tidal friction within the two closely neighboring suns: both deform each other and thereby lose rotational energy, which is transferred to the binary system. As a result, the two suns move away from each other over time and the orbital frequency decreases ($\dot{f} < 0$). Obviously, this energy transfer is greater than the energy loss due to the emitted wave that we have received.

It can be ruled out that the signal is caused by errors in the analysis program: the signal does not undergo Fourier transformation to examine its frequency bands. The reasons: Inappropriately selected parameters of the Fourier method can lead to misinterpretations. Fourier analysis is well suited to detecting strong and unmodulated signals. Detecting weak, modulated signals below the noise level requires more sophisticated communication technologies that allow the reconstruction and demodulation of existing phase modulations.

11 CONCLUSION

In this study we have explored whether atmospheric pressure records, when analysed with high-selectivity communication-engineering techniques, contain evidence of a coherent signal at the expected GW frequency of *Zeta Phoenicis*. After compensating for frequency drift and multiple phase modulations, we identify a persistent, narrow-band oscillation at 13.863 μHz whose temporal behaviour is consistent with an astrophysical origin. The detection of a modulation matching Earth's orbital period provides a directional signature, while additional sidebands suggest further dynamical structure within the source system. The improved signal-to-noise ratio achieved through phase-sensitive demodulation enables a precise measurement of the long-term frequency drift, yielding a prediction for the binary's orbital period in 2026.

Several aspects of the recovered signal differ from expectations based on standard GW theory, particularly the inferred propagation speed and the strong response of atmospheric pressure. These discrepancies highlight the need for further investigation, both observational and theoretical, into the behaviour of ultra-low-frequency waves and their coupling to terrestrial media. Nonetheless, the methodology presented here – combining coherent integration, superheterodyne demodulation, and long-baseline geophysical data – demonstrates a promising framework for detecting weak, structured signals in the microhertz regime and may serve as a foundation for future studies of continuous GW sources beyond the reach of conventional detectors.

12 METHODS

Data Acquisition: Atmospheric pressure data were obtained from the German Weather Service (DWD 2021), comprising hourly measurements from over 100 barometric stations across Germany between 2000 and 2020. Only stations with at least ten years of continuous operation were included. To enhance the signal-to-noise ratio (*SNR*), pressure records were coherently summed across all stations.

Sensor Calibration: All pressure sensors used by the DWD are temperature-compensated and conform to international standards, with a measurement range of 500-1100 hPa and an accuracy of ±0.1 hPa. Instrumental drift and data gaps remain unchanged because they may influence the amplitude of the signal, but do not generate frequency-stable oscillations or phase-modulate them. Data synchronization is accurate to the second and is guaranteed by the DWD.

Sampling: The air pressure is not measured continuously, but at fixed time intervals of, for example, T_s = 1 hour. The inverse of T_s is called the sampling frequency f_s. Although the signal does not pass through an analog low-pass filter with a cutoff frequency of $0.5 f_s$, aliasing effects are virtually eliminated when sampling atmospheric pressure hourly. This is especially true for f < 15 μHz, because the amplitudes in the lowest range are at least a factor of 10^5 higher than the spectral lines and the noise in the high frequency range (f > 100 μHz).

Signal Processing: Since we are only looking for phase-modulated (PM) signals (Haykin 2001), we apply a well-known demodulation method similar to that used in Betz (2013). The method iteratively identifies and compensates for constant modulation frequencies and

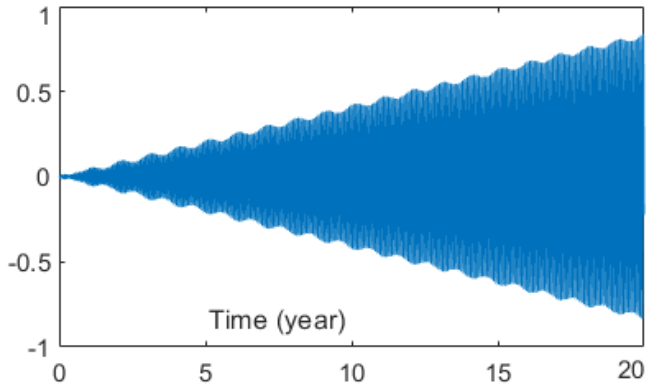

Figure 8. Integrated amplitude of a phase-modulated signal. The ripple in the envelope is caused by alternating constructive and destructive interference of the carrier frequency and sidebands. Without modulation, the amplitude increase would be linear.

concentrates the signal energy in a narrow spectral line. Unlike conventional FFT-based spectral methods, this approach preserves phase information and enables the detection of weak, phase-modulated signals below the noise threshold.

Frequency Resolution: Figure 1 shows that the frequency resolution should be better than 1 nHz. Therefore, we chose 20 years as the minimum observation time $T_{\min}$, which corresponds to the uncertainty principle $T_{\min} \cdot \Delta f \geq 0.5$ (Küpfmüller 1993). This long-term integration enables the detection of modulation periods ranging from months to decades. The frequency drift of the signals is smaller than the bandwidth of the method and can be measured and compensated using a standard superheterodyne receiver.

12.1 Coherent Signal Integration

A phase sensitive integrator acts as an extremely narrow band filter with selectable frequency and a "memory" for the phase of already processed data. This makes it insensitive to interference. Digital data is a sequence of samples z_n, z_{n+1}, z_{n+2},... , which are measured at fixed intervals (sampling time T_s). A sinusoidal signal of a given frequency f can be easily detected in this data if, for example, sampling is performed at exactly four times the frequency. This freedom is rarely available; in most cases, T_s is fixed. Then the phase angle increases by $\alpha = 2\pi f T_s$ with each measurement.

One solution for detecting the sinusoidal signal is to construct an oscillator with exactly this frequency f and feed in the digital data. If the phase is correct, the energy supply increases the amplitude of the oscillator. If the phase is opposite, the amplitude of the oscillator decreases. If this oscillator is fed with noise, the amplitude fluctuates irregularly around a mean value.

We program the oscillator with the following two CORDIC equations, which we calculate alternately:

$$x_{n+1} = cos(\alpha)x_n + sin(\alpha)y_n + z_n \quad (7)$$

$$y_{n+1} = cos(\alpha)y_n - sin(\alpha)x_n \quad (8)$$

The choice of parameters determines the sequence of calculated values x_n and y_n:

Without an injected signal ($z_n = 0$) and with initial values $x_1 = 0$ and $y_1 = 1$, the two equations calculate a table of values for $x = sin(2\pi t f)$ and $y = cos(2\pi t f)$. The amplitudes are constant.

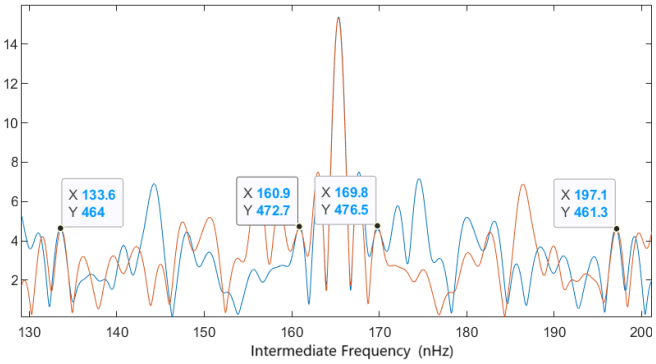

Figure 9. Superposition of the spectrum of the area surrounding the signal at the central frequency $f_{IF} = 165$ nHz with its mirror image (high and low frequencies are interchanged with respect to f_{IF}). Significant similarities are marked. These might be the sidebands caused by a modulation.

Setting $x_1 = y_1 = 0$ and feeding a monochromatic signal z_n of frequency f, the equations calculate an oscillation with frequency f, whose amplitude increases proportionally in time. The difference in phase between the signal and the oscillator disappears after a few oscillations.

If the programmed and injected frequency differ or if the phase or amplitude of the injected signal z_n changes, the output signal of the integrator varies and the linear increase of the envelope is lost. If the signal is in phase opposition, the output signal decreases proportionally to time.

If we feed a phase- or frequency-modulated signal z_n, the envelope changes in rhythm with the modulation frequency (Figure 8).

If noise is fed in, the equations calculate an oscillation, whose frequency fluctuates around f and whose amplitude varies irregularly.

Figure 8 shows a typical result when the integrator processes a signal that is phase modulated (PM) with a very small modulation index $\eta \approx 10^{-4}$. This signal consists of the carrier frequency f_0 and the two adjacent sidebands $f_0 - f_{mod}$ and $f_0 + f_{mod}$. It is difficult to measure this weak PM using other methods because the amplitudes of the sidebands are much smaller than the amplitude of the carrier.

12.2 How to find modulation frequencies

Modulating a carrier frequency f_0 with f_{mod} generates (at least) two sideband frequencies at $f_0 - f_{mod}$ and $f_0 + f_{mod}$. These are often difficult to detect in the spectrum when signals are weak and noisy. Identification is made easier by superimposing two spectra (image and mirror image) and searching for symmetries (Figure 9). If the Weaver method (Waever 1956) is used to shift the frequency of the signal, a sign change is sufficient to generate the mirror spectrum.

Since random coincidences can also be found in the noise, each “suspicious” modulation frequency must be confirmed using the method described in Weidner (2025).

12.3 Phase modulation needs bandwidth

If a signal is phase-modulated with multiple frequencies, the spectrum can look like noise (Figure 10, left side). The larger the modulation indices η, the more bandwidth the signal requires. A good demodulator is needed to identify the sideband frequencies in the noise and to decipher such a broadband signal. If the signal is processed with insufficient bandwidth, demodulation will fail.

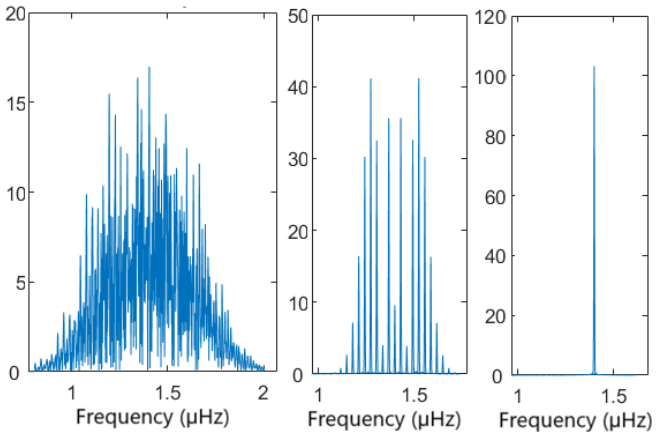

Figure 10. Left: Spectrum of the signal after the preprocessor has reduced the frequency from 13.86 μHz to 1.4 μHz. The signal is modulated as specified in Table 2. No additional noise! Middle: Spectrum with f_{mod} = 31.69 nHz alone. Right: Spectrum of the unmodulated signal. The total energy is identical in each case, and the carrier frequency is 1.4 μHz in each case.

The middle image in Figure 10 shows how many lines the spectrum is split into, even though the carrier frequency is phase-modulated with a *single* frequency. The modulation index η determines the amplitude of each line of the frequency bundle. The spectrum shows too little information to demodulate the signal because the magnitude formation inside FFT cancels out the phases of the lines.

The right-hand image in Figure 10 shows the amplitude increase of the carrier frequency when all PM is eliminated. This difference can also be seen when comparing Figures 1 and 5.

13 COMPETING INTERESTS

All investigations, including coding, were carried out by H. Weidner, who is also the sole author. The author declares no conflict of interest.

14 FUNDING

The author declares no funding.

15 AVAILABILITY OF PROGRAMS AND DATA

The German Weather Service (DWD 2021) stores historical measurement results from German weather stations (raw data). The summed, error-corrected barometer files are also available from the author upon request.

The homodyne detection code was written in MATLAB R2020a. The code (ZP22.m) and the datasets (yDWD.mat) are available in the github repository:
https://github.com/herbertweidner/cGW/tree/main

The programs will be explained by the author upon request.

References

Betz, W., 2021, The Navstar Global Positioning System, Wiley, https://doi.org/10.1002/9781119458449.ch3

Calculate radial velocities of the GBT, https://www.gb.nrao.edu/GBT/setups/radvelcalc.html

Colors of noise, https://en.wikipedia.org/wiki/Colors_of_noise

DWD, https://opendata.dwd.de/climate_environment/CDC/observations_germany

Hartmann T., Wenzel H., 1995, The HW95 tidal potential catalogue, https://publikationen.bibliothek.kit.edu/160395

Haykin, S., 2001, Communication Systems. Wiley. p. 107, ISBN 0-471-17869-1.

Küpfmüller K., Kohn G., 1993, Theoretische Elektrotechnik und Elektronik: Eine Einführung, ISBN 978-3540565000

Simbad zet Phe – Double or Multiple Star, https://simbad.cds.unistra.fr/simbad/sim-ref?bibcode=2004AcA....54..207K

Southworth J., 2020, Rediscussion of eclipsing binaries. Paper I. The totally-eclipsing B-type system Zeta Phoenicis, https://arxiv.org/pdf/2012.05559

Weaver D., A third method of generation and detection of single-sideband signals, Proceedings of the IRE, 1956, pp. 1703-5.

Weidner H., 2025, Coherent Low-Frequency Atmospheric Pressure Oscillations of Extraterrestrial Origin? in press (RASTI)

This paper has been typeset from a TEX/LATEX file prepared by the author.